

Modification of perhydropolysilazane with aluminum hydride: Preparation of poly(aluminasilazane)s and their conversion into Si–Al–N–C ceramics

Ryoji Toyoda^a, Satoshi Kitaoka^b, Yoshiyuki Sugahara^{a,*}

^a Department of Applied Chemistry, School of Science and Engineering, Waseda University, Ohkubo-3, Shinjuku-ku, Tokyo 169-8555, Japan

^b Japan Fine Ceramics Center, Atsuta, Nagoya 456-8587, Japan

Received 30 December 2006; received in revised form 28 May 2007; accepted 2 June 2007

Available online 27 September 2007

Abstract

Perhydropolysilazane (PHPS) was modified with trimethylamine–alane adduct, $\text{AlH}_3 \cdot \text{NMe}_3$, with two nominal Si/Al molar ratios (1 and 5), and the resulting poly(aluminasilazane)s were pyrolyzed under an N_2 atmosphere. Poly(aluminasilazane) with a nominal Si/Al molar ratio of 5 (PAS5) was insoluble because of the formation of cross-link points *via* dehydrocoupling. In the system with a nominal Si/Al molar ratio of 1 (PAS1), on the contrary, $\text{AlH}_3 \cdot \text{NMe}_3$ cleaved the Si–N bonds in addition to forming Al–N bonds, drastically modifying the Si–N backbone of PHPS. In addition, a large portion of aluminium was lost in the PAS1 preparation. Thermogravimetric analysis revealed that PAS5 exhibited a ceramic yield of 78% up to 900 °C, while the ceramic yield for PAS1 was 61%. The XRD patterns of the pyrolyzed residues from PAS1 and PAS5 suggest the formation of a 2H wurtzite-type compound and silicon nitride.

© 2007 Elsevier Ltd. All rights reserved.

Keywords: Precursors-organic; Composites; X-ray methods; Carbides; Nitrides

1. Introduction

The pyrolytic route, the organic-to-inorganic conversion of organometallic compounds into non-oxide ceramic materials, provides an interesting approach to the fabrication of nitride, carbide, oxynitride, and oxycarbide ceramics.^{1–4} If the precursors are soluble in organic solvents or fusible within a moderate temperature range, the pyrolytic route offers potential for a variety of applications, including use in fibers and coating preparations,^{1,5} in near-net shaping,⁶ and as a binder in the conventional powder process.⁷ Besides solubility and/or fusibility, relatively high ceramic yields are required to obtain non-porous bodies.¹ These two requirements impose limits, however, on the possible variations in precursor structures.

Poly(silazane)s, which possess Si–N backbones, have been known for decades as precursors for Si–N(–C) ceramics,⁸ in addition to their recent use as precursors for silica⁹ and silica-based hybrids.¹⁰ Among poly(silazane)s, perhydropolysilazane (PHPS), prepared *via* ammonolysis of the pyridine adduct of H_2SiCl_2 , is known to be an attractive soluble precursor with a relatively high-ceramic yield.⁴ PHPS has been utilized for Si_3N_4 -based composites, and the reactivity of SiH and NH groups in PHPS has been used to introduce different metals into precursor structures; modified PHPS has been employed for the preparation of Si–B–C–N(O),^{11–14} Si–Al–O–N,¹⁵ Si–Y–(C)–N–O,^{16–18} Si–Y–Ti–C–N–O,¹⁹ and Si–Ti–N^{20,21} ceramics. Since Al–Si–C–N ceramics are extremely attractive,²² there have been various studies on the preparation of poly(aluminasilazane)s as precursors for Al–Si–C–N ceramics.^{22–38} To the best of our knowledge, the use of PHPS in poly(aluminasilazane)s preparations has been very limited.^{15,38}

We report here the preparation of Si–Al–N–C precursors in the form of poly(aluminasilazane)s through modification of

* Corresponding author at: Department of Applied Chemistry, School of Science and Engineering, Waseda University, Ohkubo-3, Shinjuku-ku, Tokyo 169-8555, Japan.

E-mail address: ys6546@waseda.jp (Y. Sugahara).

PHPS. It is known that the N–H groups in poly(silazane)s can undergo dehydrocoupling with Al–H groups,³⁹ and this type of reaction was employed for reactions between $\text{AlH}_3 \cdot \text{NMe}_3$ and $\text{Si}(\text{NHMe})_4$ ²⁵ and between $(\text{HAlN}^i\text{Pr})_m$ and $[\text{MeSi}(\text{H})\text{NH}]_n$.^{28,30} It appears to be possible, therefore, to modify PHPS with compounds possessing Al–H groups *via* dehydrocoupling. In this study, we employed trimethylamine–alane adduct, $\text{AlH}_3 \cdot \text{NMe}_3$, and prepared poly(aluminasilazane)s with two nominal ratios ($\text{Si}/\text{Al}=1$ and 5). The structures of the modified PHPS are proposed based on spectroscopic characterization. The process of their conversion into ceramic residues and characterizations of the pyrolyzed residues are also presented.

2. Experimental Procedure

2.1. Instrumentation

Infra-red (IR) spectra were recorded on a Perkin-Elmer IR-1640 by the mull method with hexachloro,1,3-butadiene (hcb). Nuclear magnetic resonance (NMR) analysis of the precursors (CDCl_3 solvent) was performed using a JEOL JNM-LA-500 spectrometer at 499.10 MHz (^1H), 129.95 MHz (^{27}Al), and 99.05 MHz (^{29}Si). For ^{29}Si NMR, the DEPT (distortionless enhancement by polarization transfer) sequence technique⁴⁰ was also applied. The gases evolved during the synthesis were investigated using a Shimadzu GC-8A gas chromatograph equipped with a thermal conductivity detector and a JEOL JMS-AMSUN200/300 gas chromatograph/mass spectrometer. The amounts of silicon and aluminum were determined by inductively coupled emission spectrometry (ICP; Seiko Instruments SPS7000) after dissolution of about 10 mg of the precursors in 5 mL of hot 10 mol L^{-1} NaOH. The amounts of hydrogen, carbon and nitrogen were determined by an internal service at the Waseda University Materials Characterization Center.

Pyrolysis behavior was investigated by thermogravimetry (TG) using a Perkin-Elmer TGA-7 under Ar flow (100 mL/min) with a heating rate of $10^\circ\text{C}/\text{min}$ up to 900°C . Coupled TG/mass spectrometric analysis (TG/MS) was performed with a Rigaku TG-8120 thermobalance under He flow (30 mL/min) with a heating rate of $10^\circ\text{C}/\text{min}$. The thermobalance was connected with a Shimadzu GCMS-QP5050A spectrometer *via* a stainless-steel capillary. Mass spectra were obtained with an ionization energy of 70 eV in the range from 10 to 1000 amu.

The crystalline phases in pyrolyzed residues were identified using a Rigaku RINT-2500 diffractometer with monochromated $\text{Cu K}\alpha$ radiation (40 kV, 30 mA). The amounts of silicon and aluminum in the pyrolyzed residues were determined by ICP using the aforementioned instrument. For ICP measurements, about 15 mg of a pyrolyzed residue was fused with about 1 g of Na_2CO_3 at around 1000°C for at least 30 min. The amounts of carbon, nitrogen, and oxygen in the pyrolyzed residues were determined using a LECO TC-436 instrument for nitrogen and oxygen and a LECO CS-444LS instrument for carbon. The morphology of the pyrolyzed residues was investigated using a Hitachi S-4500S scanning electron microscope.

2.2. Preparation and pyrolysis of the precursors

All the procedures were performed based on the standard Schlenk techniques in a protective nitrogen atmosphere⁴¹ or in a glove box filled with nitrogen. Xylene was dried over Na prior to use. PHPS [Clariant (Japan), N-N310; IR (hcb, cm^{-1} , Fig. 1b): 3374 ($\nu_{\text{N-H}}$), 2954, 2900 ($\nu_{\text{C-H}}$), 2162 ($\nu_{\text{Si-H}}$), 1406 ($\nu_{\text{Si-C-Si}}$), 1250 ($\nu_{\text{Si-CH}_3}$), 1180 ($\delta_{\text{N-H}}$), 760–1100 ($\nu_{\text{Si-N}}$); elemental contents (mass%) Si, 62.2; N, 25.0; O, 0.4; C, 4.5] was used after dehydration with a 3A molecular sieve. $\text{AlH}_3 \cdot \text{NMe}_3$ was prepared by a procedure described in a previous study.⁴² Poly(aluminasilazane)s were prepared at nominal Si/Al molar ratios of 1 and 5. A xylene solution of PHPS (20 mass%) was cooled to 0°C , and $\text{AlH}_3 \cdot \text{NMe}_3$ was added quickly. The resultant mixture was stirred at 0°C for 1 h and then stirred further at ambient temperature for 4 h. A portion of the gases evolved during synthesis was introduced into a container for further characterization. The removal of volatiles by distillation under reduced pressure gave white powders for both $\text{Si}/\text{Al}=1$ and 5. Special care was required in the PAS1 preparation, because flammable silane formed during the synthesis operation (*vide infra*).

A precursor was placed in a BN boat, and entered into an Al_2O_3 tube filled with nitrogen and pyrolyzed at 1400, 1500, and 1600°C for 1 h under nitrogen flow (100 mL/min). The heating and cooling rate was $5^\circ\text{C}/\text{min}$.

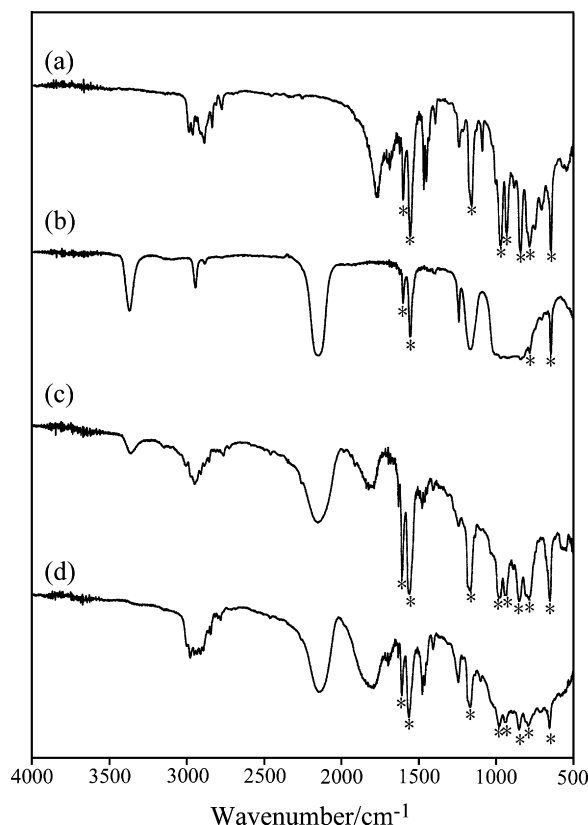


Fig. 1. IR spectra of (a) $\text{H}_3\text{Al} \cdot \text{NMe}_3$, (b) PHPS, (c) PAS5, and (d) PAS1. The bands marked by asterisks are due to hexachloro,1,3-butadiene (hcb).

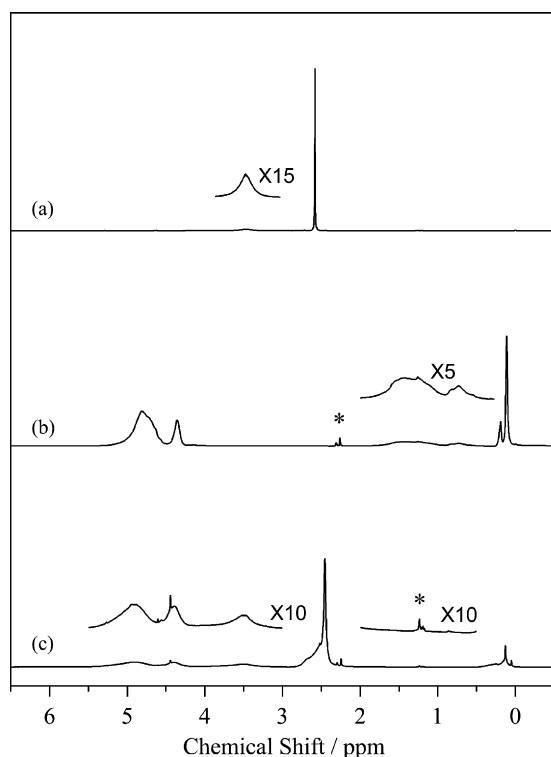


Fig. 2. ^1H NMR spectra of (a) $\text{H}_3\text{Al}\cdot\text{NMe}_3$, (b) PHPS, and (c) PAS1. The signals marked by asterisks are due to solvent (toluene).

3. Results and discussion

3.1. Characterization of precursors

Gelation occurred only for PAS5 (nominal Si/Al molar ratio of 5). PAS1 (nominal Si/Al molar ratio of 1) was soluble in organic solvents such as tetrahydrofuran and chloroform, while PAS5 was insoluble.

Fig. 1 demonstrates the IR spectra of PHPS, PAS1, and PAS5. Compared to the spectrum of PHPS, the relative intensity of the $\nu_{(\text{N-H})}$ band at around 3370 cm^{-1} ⁴³ decreases in the spectrum of PAS5. With a larger relative amount of $\text{AlH}_3\cdot\text{NMe}_3$ (nominal Si/Al molar ratio of 1, PAS1), the $\nu_{(\text{N-H})}$ band completely disappears. In the spectra of both PAS1 and PAS5, the $\nu_{\text{Al-H}}$ bands (1798 cm^{-1}), which show shifts from the $\nu_{\text{Al-H}}$ band position of $\text{AlH}_3\cdot\text{NMe}_3$ (1778 cm^{-1}), and the $\nu_{\text{Si-H}}$ bands (PAS1, 2140 cm^{-1} ; PAS5, 2154 cm^{-1})⁴³ are clearly observed.

Fig. 2 demonstrates the ^1H NMR spectra of $\text{AlH}_3\cdot\text{NMe}_3$, PHPS, and PAS1. NMR characterization of insoluble PAS5 was impossible. Compared to the spectrum of PHPS (Fig. 2b), signals for the AlH groups (3.49 ppm) and NMe_3 [$\text{N}(\text{CH}_3)_3$] (2.45 ppm)⁴¹ appear in the spectrum of PAS1 (Fig. 2c). While a broad peak ascribed to NH groups is observed at 0.6–1.6 ppm in the spectrum of PHPS, no NH signal is detected in the spectrum of PAS1, which is in accordance with the IR results. In addition, the intensities of the signals due to $\equiv\text{SiMe}$ ($\equiv\text{SiCH}_3$) groups in PHPS (0.11 and 0.25 ppm)¹⁷ decrease significantly. The profiles of the signals due to SiH groups (~ 4.4 ppm, NSiH_3 ; ~ 4.9 ppm, $\text{N}_3\text{SiH}/\text{N}_2\text{SiH}_2$)¹⁷ show a slight difference between the spectra of PHPS and PAS1, and the intensity ratios of the 4.4-ppm sig-

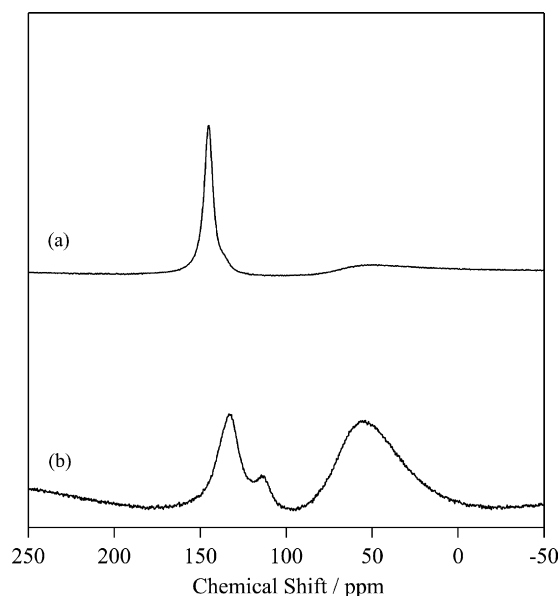


Fig. 3. ^{27}Al NMR spectra of (a) $\text{H}_3\text{Al}\cdot\text{NMe}_3$ and (b) PAS1.

nal and the 4.9-ppm signal ($I_{4.4}/I_{4.9}$) increase upon the treatment with $\text{AlH}_3\cdot\text{NMe}_3$.

The ^{27}Al NMR spectrum of PAS1 is shown in Fig. 3. In the spectrum of PAS1, three signals are observed at 56, 113, and 133 ppm. The signals at 56 and 113 ppm are ascribed to the AlN_5 ²⁷ and AlN_4 ⁴⁴ environments, respectively. Since several signals were reported near 133 ppm, the HAlN_3 environments in cage-type $(\text{HAlNR})_n$ at ~ 130 ppm^{45,46} and the H_2AlN_2 and HAlN_3 environments at 116–120 ppm,⁴⁷ the 133-ppm signal can be ascribed to the $\text{H}_x\text{AlN}_{4-x}$ environments. Since NMe_3 is still detected by ^1H NMR, Al-NMe_3 linkage appears to remain in these environments, at least in part.

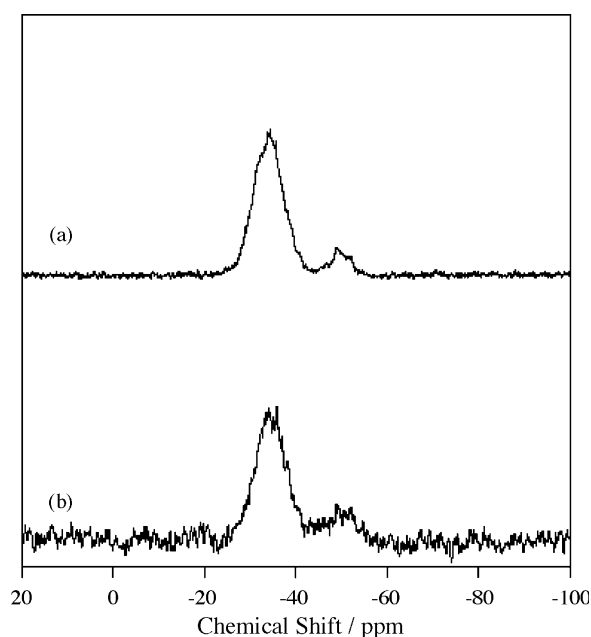


Fig. 4. ^{29}Si NMR spectra of (a) PHPS and (b) PAS1.

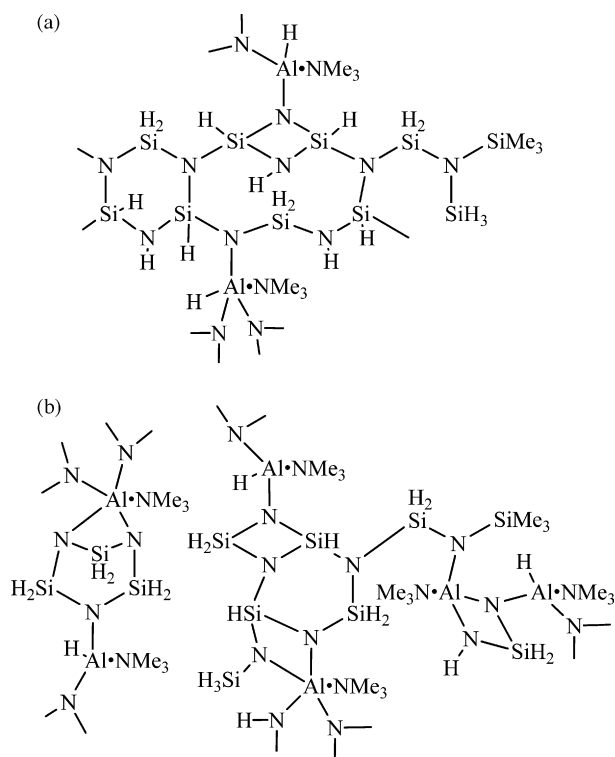


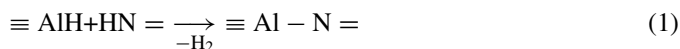
Fig. 5. Proposed structures of (a) PAS5 and (b) PAS1.

Silicon-29 NMR provides further information on the Si environments of PAS1 (Fig. 4). Both PHPS and PAS1 exhibit two broad signals, one of which is a signal (centered at around -50 ppm) ascribable to an NSiH_3 environment.¹⁸ The other signal is deconvoluted into two signals at -35 ppm (N_3SiH) and -33 ppm (N_2SiH_2), as confirmed by DEPT measurements with different pulse angles (not shown). The profile changes slightly upon reaction with $\text{AlH}_3\cdot\text{NMe}_3$, as was expected from the ^1H NMR results.

3.2. Reaction mechanism

When a smaller amount of $\text{AlH}_3\cdot\text{NMe}_3$ was reacted with PHPS (nominal Si/Al molar ratio of 5), the resulting product (PAS5) was a gel that was insoluble in organic solvents. With the use of a larger amount of $\text{AlH}_3\cdot\text{NMe}_3$, on the contrary, a soluble product (PAS1) was formed. It seems, therefore, that the addition of $\text{AlH}_3\cdot\text{NMe}_3$ resulted in the formation of an insoluble cross-linked network only when the amount of $\text{AlH}_3\cdot\text{NMe}_3$ employed was small.

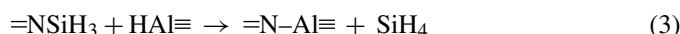
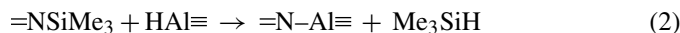
The gases captured during the preparation of PAS1 were identified by GC and GC/MS analyses as H_2 , SiH_4 , MeSiH_3 , and NMe_3 . The formation of hydrogen and the loss of the NH groups (as shown by the IR and NMR results) indicate that the following dehydrocoupling had occur, as anticipated based on previous reports^{25,39}:



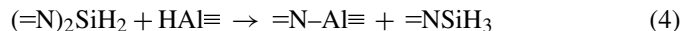
$\text{AlH}_3\cdot\text{NMe}_3$ can form a maximum of three Al–N bonds *via* dehydrocoupling, and the additional coordination of nitrogen

(in the PHPS structure and/or NMe_3) leads to the formation of AlN_4 and AlN_5 environments. The presence of the AlN_4 and AlN_5 environments as revealed by ^{27}Al NMR, therefore, clearly demonstrates that $\text{AlH}_3\cdot\text{NMe}_3$ acts as a cross-linking reagent. Since the shift of the $\nu_{(\text{Al}-\text{H})}$ band to a higher wave number was reported for dehydrocoupling of $\text{AlH}_3\cdot\text{NMe}_3$ with the NH groups,³⁹ the observed $\nu_{(\text{Al}-\text{H})}$ band shift indicates the formation of $\text{H}_x\text{AlN}_{4-x}$ environments, whose presence is demonstrated by the ^{27}Al NMR results, *via* the same type of dehydrocoupling.

Since $=\text{NSiMe}_3$ and $=\text{NSiH}_3$ groups are present in PHPS,¹⁷ the formation of SiH_4 and Me_3SiH reveals the cleavage of the Si–N bonds by the AlH groups in the following manner³⁹:



The reaction (Eq. (2)) shows good consistency with the decrease in the $\equiv\text{SiMe}$ environment after the reaction (^1H NMR, Fig. 2). No corresponding change is observed, however, for SiH_4 formation in the ^1H NMR results; the number of $-\text{SiH}_3(=\text{NSiH}_3)$ groups relative to numbers of the $=\text{SiH}_2[(=\text{N})_2\text{SiH}_2]$ and $\equiv\text{SiH}[(=\text{N})_3\text{SiH}]$ groups increases upon treatment with $\text{AlH}_3\cdot\text{NMe}_3$. This appears to be ascribable partly to the simultaneous appearance and disappearance of the $=\text{NSiH}_3$ environment. The $=\text{NSiH}_3$ environment is consumed to form SiH_4 *via* the reaction (Eq. (3)) and is also generated from the $(=\text{N}_2)\text{SiH}_2$ environment *via* the following reaction:



The following reaction is similarly expected to occur:

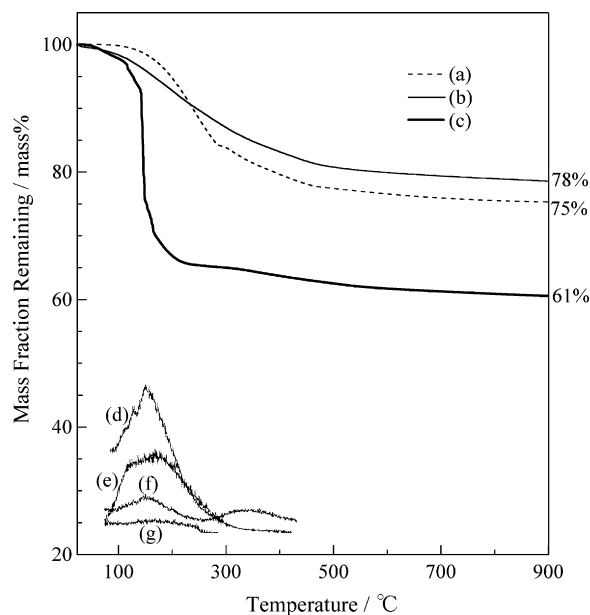
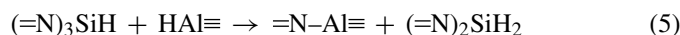


Fig. 6. TG curves of (a) PHPS, (b) PAS5, and (c) PAS1 under He flow. The variations in the intensity of the fragments during simultaneous TG–MS analysis of PAS1 [curve(c)] are also shown; curves (d–g) show fragments at m/e 58, m/e 30, m/e 15 and m/e 73, respectively.

Table 1
Compositional characteristics of pyrolyzed products

Precursor	Pyrolytic condition	Ceramic yield (mass%)	Composition (mass%)						Empirical formula	Si/Al
			Si	Al	N	C	O	Total		
PAS5	1500 °C, N ₂ , 1 h	74	53.4	10.8	26.2	9.8	1.1	101.3	Si _{1.0} Al _{0.21} N _{0.98} C _{0.43} O _{0.04}	4.75
PAS1	1400 °C, N ₂ , 1 h	59	31.3	27.6	25.0	8.2	1.5	93.6	Si _{1.0} Al _{0.51} N _{0.63} H _{6.0} C _{1.2}	1.11
	1500 °C, N ₂ , 1 h	59	32.7	29.1	24.1	8.6	1.7	96.2	Si _{1.0} Al _{0.93} N _{1.5} C _{0.62} O _{0.09}	1.08
	1600 °C, N ₂ , 1 h	58	32.6	28.8	24.1	9.3	1.8	96.6%	Si _{1.0} Al _{0.92} N _{1.5} C _{0.67} O _{0.10}	1.09

It is worth noting that these two reactions (Eqs. (4) and (5)) do not involve gas evolution but lead to a reduction of molecular mass.

As the above discussion suggests, the cleavage of the Si–N bonds seems to account for the formation of soluble oligomers during PAS1 preparation, despite the formation of cross-linking points *via* the dehydrocoupling reaction (Eq. (1)). Based on compositional analyses, the empirical formula for PAS1 is Si_{1.0}Al_{0.51}N_{0.63}H_{6.0}C_{1.2}. Thus, the Si/Al molar ratio in PAS1 increased to 1.97 from the nominal value (Si/Al = 1). Since Al was detected in the volatiles removed during distillation under reduced pressure, it is apparent that only a part of AlH₃·NMe₃ was reacted in PAS1 preparation. The amount of reacted AlH₃·NMe₃ is calculated from the Si/Al molar ratio (1.97) to be 50.8%, but the actual amount should be smaller when the loss of silanes (SiH₄ and Me₃SiH) is taken into consideration. The large reduction in the amount of reacted AlH₃·NMe₃ also seems to account in part for the solubility of PAS1. The empirical formula for PAS5, on the contrary, is Si_{1.0}Al_{0.21}N_{0.83}H_{4.9}C_{0.99},

indicating that the Si/Al molar ratio of PAS5 is very close to the nominal ratio (Si/Al = 5). In addition, no loss of Al-containing species was observed during distillation under reduced pressure. Thus, essentially all of AlH₃·NMe₃ is reacted and acts mainly as a cross-linking reagent to form an insoluble network.

Si–N bond cleavage is apparent only during the synthesis of PAS1. Since the IR results indicate a complete loss of the NH groups in PAS1, whose preparation involves a larger amount of AlH₃·NMe₃, it is reasonable to assume that all the NH groups undergo dehydrocoupling, suggesting that the AlH groups remain present in considerable numbers. Thus, attacks by the AlH groups on the Si–N bonds must occur frequently. When the nominal Si/Al molar ratio is 5, on the contrary, the number of NH groups is larger than that of AlH groups in starting compounds. Thus, a large portion of the AlH groups must be consumed by dehydrocoupling. In the PAS5 structure, however, both NH groups and AlH groups are present, as shown by the IR results. It is therefore assumed that the remaining AlH groups are positioned at immobilized sites present in the three-dimensional network. Thus, the Si–N bond cleavage is limited in PAS5 preparation, and AlH₃·NMe₃ acts mainly as a cross-link reagent to form an insoluble cross-linked network, despite the smaller AlH₃·NMe₃ content. It is therefore reasonable to assume that the AlN₄ and AlN₅ environments, which are present in PAS1, are also present in the PAS5 structure, although ²⁷Al NMR information is lacking. Structural models of PAS1 and PAS5 proposed based on this discussion are shown in Fig. 5.

3.3. Pyrolysis of the precursors

Fig. 6 shows TG curves for PHPS, PAS1, and PAS5 up to 900 °C at which conversion of the precursors into ceramic residues is essentially completed. The ceramic yield of PAS1 (61%) is lower than that of unmodified PHPS (75%). A large mass loss, which is not observed in the TG curve of PHPS, is present at around 100–200 °C in the TG curve of PAS1. TG–MS analysis of PAS1 (Fig. 6) reveals evolution of SiH₄ (as shown by the fragment at *m/e* 30) and Me₃SiH (*m/e* 73), in addition to that of NMe₃ (*m/e* 58; although NMe₃ exhibits a weak fragment at *m/e* 30, the contribution of NMe₃ to the fragment at *m/e* 30 is expected to be small). The formation of SiH₄ and Me₃SiH is observed up to ~300 °C, and the temperature range at which these silanes are formed mostly overlaps the steep mass loss. Since the AlH groups are present in PAS1 with no remaining NH groups (as shown by IR; Fig. 1), further Si–N bond cleav-

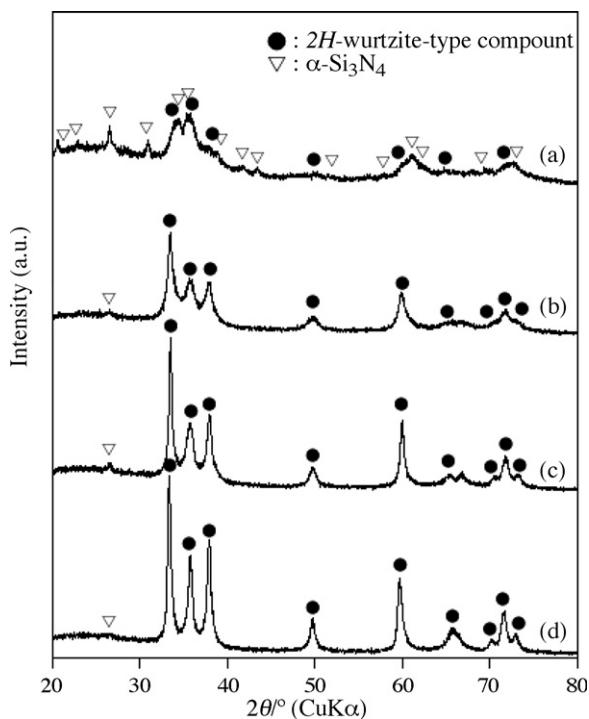


Fig. 7. XRD patterns of the residues pyrolyzed under N₂ flow for 1 h: (a) PAS5 pyrolyzed at 1500 °C, (b) PAS1 pyrolyzed at 1400 °C, (c) PAS1 pyrolyzed at 1500 °C, and (d) PAS1 pyrolyzed at 1600 °C.

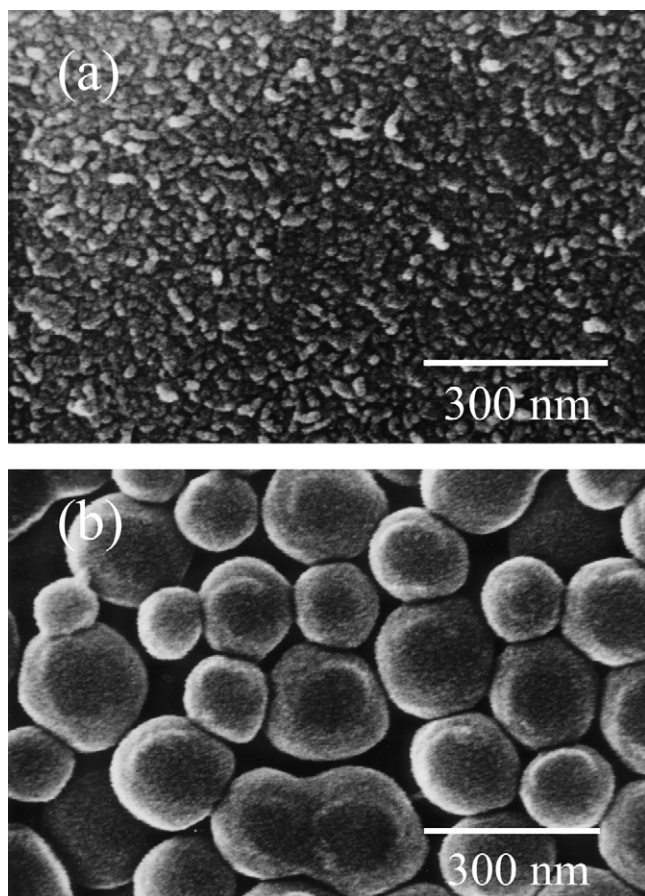


Fig. 8. Scanning electron micrographs of the residues pyrolyzed under N_2 flow at $1500^\circ C$ for 1 h: (a) from PAS5 and (b) from PAS1.

age occurs in this temperature range to reduce the ceramic yield. Although the fragment at m/e 15 below $\sim 300^\circ C$ could originate from methyl groups in evolved gases, the fragment at m/e 15 in the higher temperature range where gas evolution is essentially completed ($>300^\circ C$) should be ascribed mainly to CH_4 formation from the remaining $\equiv SiCH_3$ groups in a cross-linked network. The ceramic yield of PAS5 (78%) is slightly larger than that of PHPS, but it is lower than the ceramic yield range expected for cross-linked PHPS. TG–MS analysis revealed that no silanes had evolved, but NMe_3 was clearly detected. Thus, this moderate ceramic yield is partly ascribable to the presence of NMe_3 in the structure.

Table 1 lists the ceramic yields for the pyrolysis. The ceramic yield of PAS5 (74% at $1500^\circ C$) is larger than the corresponding value for PAS1 (59%), which is consistent with the TG results. The compositions of the pyrolyzed residues are also shown in Table 1. The Si/Al molar ratio of the ceramic residue from PAS5 is essentially the same as that of the PAS5 precursor. The Si/Al molar ratios of the pyrolyzed residues from PAS1 (1.06–1.11), on the contrary, are much smaller than that of the PAS1 precursor (1.97). This is consistent with the evolution of silanes at low temperatures, as shown by the TG–MS analysis.

The XRD patterns of the pyrolyzed residues are shown in Fig. 7. The residue obtained by pyrolyzing PAS5 at $1500^\circ C$ exhibits broad reflections ascribable to a $2H$ wurtzite-type

compound⁴⁸ and α - Si_3N_4 . The XRD patterns of the pyrolyzed residues from PAS1 also consist of reflections due to the $2H$ wurtzite-type compound and α - Si_3N_4 . The variation in pyrolysis temperatures (1400 – $1600^\circ C$) does not affect the XRD profiles to any considerable extent. The $2H$ wurtzite-type compound in the Si–Al–N–C system could be a mixture of AlN and $2H$ -SiC or an AlN/SiC solid solution (or a mixture of solid solutions).^{48,49} The XRD reflections are too broad, however, to permit analysis of the line shapes or to determine the lattice parameters.

Fig. 8 shows scanning electron micrographs of the residues pyrolyzed at $1500^\circ C$. The pyrolyzed residue from PAS5 consists of fine particles (20–40 nm in diameter), while much larger particles are observed in the pyrolyzed residue from PAS1. The particle size estimated by XRD reflection broadening indicates, however, that the average particle size of the residue obtained by pyrolyzing PAS1 at $1500^\circ C$ is ~ 37 nm. The difference between the observed (SEM) and estimated (XRD) particle sizes can be explained by the fact that the observed particles are aggregates of crystallites.

4. Conclusions

PHPS has been modified with $AlH_3 \cdot NMe_3$ to form poly(aluminasilazane)s. $AlH_3 \cdot NMe_3$ acts as a cross-link reagent via a dehydrocoupling reaction, but the AlH groups also cleave the Si–N bonds. Poly(aluminasilazane) prepared with a nominal Si/Al molar ratio of 5 (PAS5) is insoluble, indicating that $AlH_3 \cdot NMe_3$ provides cross-linking points to form a three-dimensional network. Si–N bond cleavage is extremely limited during PAS5 preparation. The Si/Al molar ratio in PAS5 (4.85) is consistent with the nominal value. Poly(aluminasilazane) prepared with a nominal Si/Al molar ratio of 1 (PAS1), on the contrary, is soluble in organic solvents. Though dehydrocoupling generates AlN_5 and AlN_4 environments, the cleavage of the Si–N bonds leads to drastic changes in the Si–N backbone structure originating in PHPS and the evolution of silanes (SiH_4 and Me_3SiH). In spite of the evolution of silanes, the Si/Al molar ratio increases to 1.97 because of the loss of a considerable portion of Al in PAS1 preparation. The ceramic yield of PAS5 (78%) is higher than that of PHPS (75%), while PAS1 exhibits a lower ceramic yield (61%) due mainly to silane formation at ~ 100 – $200^\circ C$ via Si–N bond cleavage during pyrolysis. All the pyrolyzed residues mainly contain a $2H$ wurtzite-type compound with relatively small amounts of silicon nitride. The present study demonstrates that Si–N bond cleavage by the AlH groups could be involved during the modification of poly(silazane)s with molecules bearing Al–H groups. Thus, modification with aluminum hydride and related molecules should be carefully designed for both dehydrocoupling and Si–N bond cleavage.

Acknowledgment

The authors gratefully thank Prof. Kazuyuki Kuroda, Department of Applied Chemistry, Waseda University, for his valuable discussions.

References

1. Narula, C. K., *Ceramic Precursor Technology and Its Applications*. Marcel Dekker, New York, 1995.
2. Mori, Y. and Sugahara, Y., *J. Ceram. Soc. Japan*, 2006, **114**, 461.
3. Mutin, P. H., *J. Sol–Gel Sci. Technol.*, 1999, **14**, 27.
4. Kroke, E., Li, Y.-L., Konetschny, C., Lecomte, E., Fasel, C. and Riedel, R., *Mater. Sci. Eng.*, 2000, **R26**, 97.
5. Okamura, K., *Composites*, 1987, **18**, 107.
6. Greil, P., *J. Eur. Ceram. Soc.*, 1998, **18**, 1905.
7. Seyferth, D. and Czubarow, P., *Chem. Mater.*, 1994, **6**, 10.
8. Seyferth, D., Wiseman, G. H. and Prud'homme, C., *J. Am. Ceram. Soc.*, 1983, **66**, C13.
9. Kubo, T., Tadaoka, E. and Kozuka, H., *J. Mater. Res.*, 2004, **19**, 635.
10. Saito, R., *J. Polym. Sci., Part A: Polym. Chem.*, 2006, **44**, 5174.
11. Funayama, O., Kato, T., Tashiro, Y. and Isoda, T., *J. Am. Ceram. Soc.*, 1993, **76**, 717.
12. Funayama, O., Nakahara, H., Tezuka, A., Ishii, T. and Isoda, T., *J. Mater. Sci.*, 1994, **29**, 2238.
13. Funayama, O., Nakahara, H., Okoda, M., Okumura, M. and Isoda, T., *J. Mater. Sci.*, 1995, **30**, 410.
14. Funayama, O., Aoki, T. and Isoda, T., *J. Ceram. Soc. Jpn.*, 1996, **104**, 355.
15. Funayama, O., Tashiro, Y., Aoki, T. and Isoda, T., *J. Ceram. Soc. Jpn.*, 1994, **102**, 908.
16. Iwamoto, Y., Matsubara, H. and Brook, R. J., *Ceram. Trans (Ceramic Processing Science and Technology)*. The American Ceramic Society, Westerville, 1995, 193.
17. Iwamoto, Y., Kikuta, K. and Hirano, S., *J. Mater. Res.*, 1998, **13**, 353.
18. Iwamoto, Y., Kikuta, K. and Hirano, S., *J. Mater. Res.*, 1999, **14**, 1886.
19. Iwamoto, Y., Kikuta, K. and Hirano, S., *J. Mater. Res.*, 1999, **14**, 4294.
20. Iwamoto, Y., Kikuta, K. and Hirano, S., *J. Ceram. Soc. Jpn.*, 2000, **108**, 350.
21. Sato, K., Saitoh, T., Nagano, T. and Iwamoto, Y., *J. Ceram. Soc. Jpn.*, 2006, **114**, 502.
22. An, L., Wang, Y., Bharadwaj, L., Zhang, L., Fan, Y., Jiang, D., Sohn, Y., Desai, V. H., Kapat, J. and Chow, L. C., *Adv. Eng. Mater.*, 2004, **6**, 337.
23. Czekaj, C. L., Hackney, M. L. J., Hurley Jr., W. J., Interrante, L. V., Sigel, G. A., Schields, P. J. and Slack, G. A., *J. Am. Ceram. Soc.*, 1990, **73**, 352.
24. Interrante, L. V., Schmidt, W. R., Marchetti, Q. S. and Maciel, G. E., In *Synthesis and Processing of Ceramics: Scientific Issues*, ed. W. E. Rhine, T. M. Shaw, R. J. Gottschall and Y. Chen. Materials Research Society, Warrendale, PA, 1992, p. 31.
25. Löffelholz, J. and Jansen, M., *Adv. Mater.*, 1995, **7**, 289.
26. Seyferth, D., Brodt, G. and Boury, B., *J. Mater. Sci. Lett.*, 1996, **15**, 348.
27. Verdecia, G., O'Brien, K. L., Schmidt, W. R. and Apple, T. M., *Chem. Mater.*, 1998, **10**, 1003.
28. Koyama, S., Nakashima, H., Sugahara, Y. and Kuroda, K., *Chem. Lett.*, 1998, **27**, 191.
29. Boury, B. and Seyferth, D., *Appl. Organomet. Chem.*, 1999, **13**, 431.
30. Nakashima, H., Koyama, S., Kuroda, K. and Sugahara, Y., *J. Am. Ceram. Soc.*, 2002, **85**, 59.
31. Berger, F., Weinmann, M., Aldinger, F. and Muller, K., *Chem. Mater.*, 2004, **16**, 919.
32. Cheng, F., Kelly, S. M., Lefebvre, F., Clark, S., Supplit, R. and Bradley, J. S., *J. Mater. Chem.*, 2005, **15**, 772.
33. Dhamne, A., Xu, W., Fookes, B. G., Fan, Y., Zhang, L., Burton, S., Hu, J., Ford, J. and An, L., *J. Am. Ceram. Soc.*, 2005, **88**, 2415.
34. Wang, Y., An, L., Fan, Y., Zhang, L., Burton, S. and Gan, Z., *J. Am. Ceram. Soc.*, 2005, **88**, 3075.
35. Wang, Y., Fei, W. and An, L., *J. Am. Ceram. Soc.*, 2006, **89**, 1079.
36. Wang, Y., Fan, Y., Zhang, L., Zhang, W. and An, L., *Scripta Mater.*, 2006, **55**, 295.
37. Mori, Y. and Sugahara, Y., *Appl. Organomet. Chem.*, 2006, **20**, 527.
38. Mori, Y., Ueda, T., Kitaoka, S. and Sugahara, Y., *J. Ceram. Soc. Jpn.*, 2006, **114**, 497.
39. Fookan, U., Khan, M. A. and Wehmschulte, R. J., *Inorg. Chem.*, 2001, **40**, 1316.
40. Kovar, R. A. and Callaway, J. O., *Inorg. Synth.*, 1977, **17**, 36.
41. Braun, S., Kalinowski, H.-O. and Berger, S., *100 and More Basic NMR Experiments*. VCH, Weinheim, 1996.
42. Shriver, D. F. and Drezdson, M. A., *The Manipulation of Air-Sensitive Compounds (2nd ed.)*. Wiley-Interscience, New York, 1986.
43. Nakamoto, K., *Infrared and Raman Spectra of Inorganic and Coordination Compounds*. Wiley-Interscience, New York, 1997.
44. Fitzgerald, J. J., Kohl, S. D., Piedra, G., Dec, S. F. and Maciel, G. E., *Chem. Mater.*, 1994, **6**, 1915.
45. Sugahara, Y., Onuma, T., Tanegashima, O., Kuroda, K. and Kato, C., *J. Ceram. Soc. Jpn.*, 1992, **100**, 101.
46. Koyama, S., Takeda, H., Saito, Y., Sugahara, Y. and Kuroda, K., *J. Mater. Chem.*, 1996, **6**, 1055.
47. Akitt, J. W., *Prog. Nucl. Magn. Reson. Spectrosc.*, 1989, **21**, 1.
48. Cutler, I. B., Miller, P. D., Rafaniello, W., Park, K. H., Thompson, D. P. and Jack, K. H., *Nature*, 1978, **275**, 434.
49. Sugahara, Y., Sugimoto, K., Takagi, H., Kuroda, K. and Kato, C., *J. Mater. Sci. Lett.*, 1988, **7**, 795.